

Constraining global parameters of accreting black holes by modeling magnetic flares

R. W. Goosmann^{1,2}, M. Mouchet³, M. Dovčiak¹,
V. Karas¹, B. Czerny⁴, G. Ponti^{5,6}

¹ Astronomical Institute, Academy of Sciences, Boční II 1401, 14131 Prague, Czech Republic

² Observatoire de Paris, Meudon, LUTH, 5 place Jules Janssen, 92195 Meudon Cedex, France

³ Laboratoire ApC, Université Denis Diderot, 2 place Jussieu, 75251 Paris Cedex 05, France

⁴ Copernicus Astronomical Center, Bartycka 18, 00-716 Warsaw, Poland

⁵ Dipartimento di Astronomia, Università di Bologna, Via Ranzani 1, 40127, Bologna, Italy

⁶ INAF-IASF Bologna, via Gobetti 101, 40129, Bologna, Italy

Abstract

We present modeling results for the reprocessed radiation expected from magnetic flares above AGN accretion disks. Relativistic corrections for the orbital motion of the flare and for the curved space-time in the vicinity of the black hole are taken into account. We investigate the local emission spectra, as seen in a frame co-orbiting with the disk, and the observed spectra at infinity. We investigate long-term flares at different orbital phases and short-term flares for various global parameters of the accreting black hole. Particular emphasis is put on the relation between the iron $K\alpha$ line and the Compton hump as these two features can be simultaneously observed by the *Suzaku* satellite and later by *Simbol-X*.

1 Introduction

The magnetic flare model is an attractive possibility to explain the X-ray properties of accreting black holes in Active Galactic Nuclei (AGN). It was originally suggested by Galeev et al. (1979) and developed in several subsequent papers (e.g. Haardt & Maraschi 1991; Haardt et al. 1994). The flares supposedly result from reconnection events in the magnetized corona of the accretion disk. They account for the heating of the corona to a very hot (10^8 – 10^9 K) and optically thin medium. This medium explains the production of the observed primary X-ray spectrum by Compton up-scattering of soft X-ray photons coming from the accretion disk.

The flares may appear with different durations and intensities. The rapid fluctuations seen in X-ray lightcurves of AGN can be explained by the random appearance of numerous “weak” flares distributed across an accretion disk. Such a model is described in Czerny et al. (2004) and Goosmann et al. (2006). It enables to constrain global parameters of AGN by fitting their *rms* variability spectrum. But also “strong” (very intense) flares are occasionally seen in the X-ray lightcurves of some nearby Seyfert galaxies (MCG-6-30-15, Ponti et al. 2004; NGC 5548, Kaastra et al. 2004). Such flares can dominate the X-ray spectrum on time scales of thousands of seconds.

We present spectral modeling over 2–30 keV of strong X-ray flares occurring above an AGN accretion disk. We concentrate on the reprocessed component expected from the illuminated patch underneath the flare source. Our radiative transfer simulations include computations of the vertical disk structure and modifications of the spectrum by general relativistic and Doppler effects.

2 Model

We assume a compact flare source elevated to a height H above the accretion disk and emitting a primary spectrum with $F(E) \propto E^{-\alpha}$. The primary source produces an irradiated, horizontally stratified hot spot on the disk; the highest illuminating flux appears at the spot center and the lowest at the border. We solve the radiative transfer for five different concentric annuli of the hot

spot using the codes TITAN and NOAR (Dumont et al. 2000, 2003). The vertical structure of the accretion disk is computed with a new version of the code by Róžańska et al. (2002). Details of these calculations can be found in Goosmann (2006). The resulting local spectra are obtained at twenty different emission angles. These spectra are then used with the ray-tracing code KY (Dovčiak et al. 2004; Dovčiak 2004) that computes the spectral evolution seen by a distant observer. The code takes into account all effects of general relativity and the Keplerian motion of the hot spot around the black hole.

3 Spectral appearance at different orbital phases

First, we investigate the observed spectrum of the spot at different orbital phases. The following parameters for the accreting black hole are set: mass $M = 10^8 M_\odot$, dimensionless spin $a/M = 0.998$, and accretion rate (in units of the Eddington accretion rate) $\dot{m} = 0.001$; for the flare we set $\alpha = 0.9$, $H = 0.5 R_g$, with $R_g = \frac{GM}{c^2}$, and the spot radius $R_X = H \tan \theta_0$, where $\theta_0 = 60^\circ$ is the half-opening angle of the “beaming cone”. The thermal flux from the disk at the spot center, F_{disk} , is assumed to be much weaker than the flare irradiation $F_X = 144 \times F_{\text{disk}}$. The local radiative transfer calculations are conducted for a spot at a disk radius of $R = 7 R_g$. When computing the distant spectra we neglect that the local spectra change for other disk radii – we thus only emphasize the relativistic effects. We assume that the hot spot exists for a quarter of an orbit and we analyze the resulting time-integrated spectrum at four different azimuthal phases. The viewing direction of the distant observer is inclined by $i = 30^\circ$ with respect to the disk normal.

We show the resulting spectra in Fig. 1. The reprocessing features we are particularly interested in are the Compton hump and the iron $K\alpha$ line complex. In the local frame of the disk, the Compton hump is situated around 30 keV and the laboratory energy of the iron line ranges, depending on the ionization state, between 6.4 and 6.9 keV. The figure shows how the reprocessing features are shifted by gravitational energy shift and Doppler effects. The gravitational shift depends only on R while the Doppler effect also changes with the azimuthal phase. As a result of these two effects, the iron $K\alpha$ line is smeared out and the smearing becomes stronger with decreasing R . Very close to the black hole, at $R = 3 R_g$, the line is not recognizable any more. Furthermore, the relative flux between the Compton hump and the iron line maximum changes systematically and decreases with R . The closer to the black hole the spectra originate, the flatter they appear. Furthermore, light-bending effects and the frame dragging around the fast-spinning black hole are important. They induce an asymmetric shape of the relativistic transfer functions (as seen on the maps by Dovčiak 2004). The normalization of the spectrum is higher between $\phi = 135^\circ$ and $\phi = 315^\circ$ than for the other half-orbit. Also the deformation of the iron line differs between the two half-orbits.

4 Short-term flares for different system parameters

Next, we consider short-term flares. Their irradiation time is supposed to be comparable to the light-crossing time of the hot spot. Therefore, the spot re-emission evolves from the spot center, where the first incident photons arrive, to the border. The local lightcurves show a rising phase, a maximum, and a fade-out phase. We compute models changing the inclination of the observer and the global parameters of the accreting black hole. We set $a/M = 0$ and calculate reprocessing spectra for spots at disk radii of $R = 7 R_g$ and $R = 18 R_g$.

In Table 1 we show hard/soft-flux ratios $\zeta_{\text{hs}} = F[28 \text{ keV}]/F[4 \text{ keV}]$ and equivalent widths of the iron $K\alpha$ line for both the locally emitted and the far-away observed spectra of a spot passing “behind” the black hole ($\phi = 180^\circ$). The spectra are taken at the maximum of the lightcurve. For almost all local spectra we examine, the spectral hardness decreases with increasing inclination. After including the relativistic and Doppler effects, this trend is reversed for the closer-in hot-spots at $7 R_g$. Generally, the equivalent width seen by a distant observer, $EW_{\text{far}}(K\alpha)$, is diminished in comparison to the local value, $EW_{\text{loc}}(K\alpha)$, although the definition of the continuum level was made

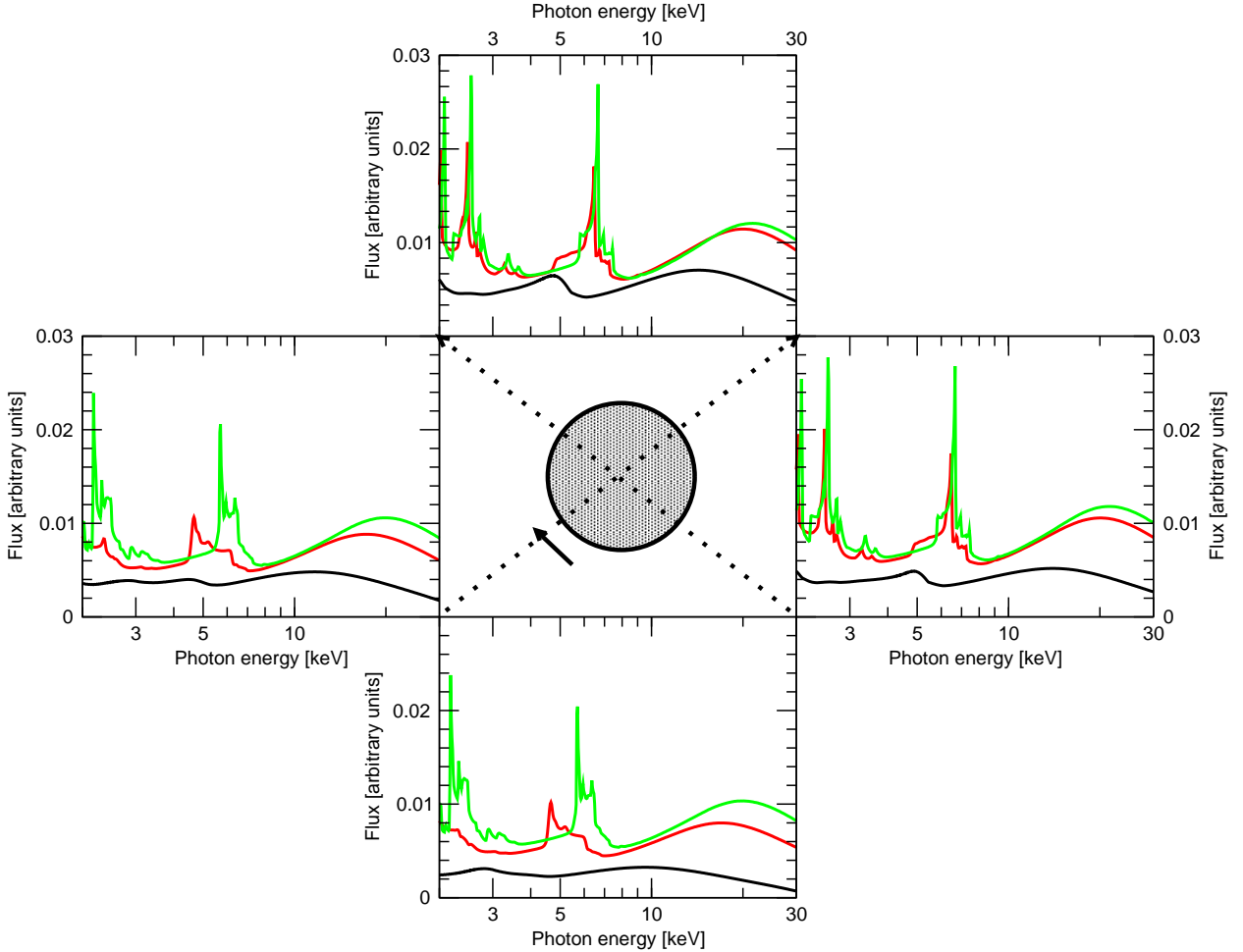


Figure 1: Time-integrated spectra seen by a distant observer for a hot spot completing a quarter of an orbit. The observer is located at the bottom of the figure and inclined by $i = 30^\circ$ with respect to the disk normal. The bottom figure hence represents the orbital phase $\phi = 0^\circ$, when the spot is at the closest approach to the observer. The disk and the black hole rotate clockwise. The curves denote spots at different disk radii: $3 R_g$ (black), $10 R_g$ (red), and $40 R_g$ (green).

by eye, which induces uncertainties. The set of parameters for $M = 10^7 M_\odot$ corresponds to the characteristics of the Seyfert galaxy MCG-6-30-15 during a strong flare (Ponti et al. 2004). In this case the ratio F_X/F_{disk} is weaker than before, which slightly hardens the reprocessed spectrum. Adding dilution by the primary radiation (primary = 1 in Table 1, primary = 0 means pure reflection) decreases the equivalent widths of the $K\alpha$ -line, as expected.

5 Discussion

There are good arguments to assume that the X-ray irradiation pattern across an AGN accretion disk is not azimuthally symmetric. Indications of this asymmetry can be found for NGC 3516 in Iwasawa et al. (2004), for NGC 5548 in Kaastra et al. (2004), or for Mrk 766 in Turner et al. (2006). The authors use timing analysis of spectral data from *XMM-Newton* and *Chandra* to constrain orbital motions of localized X-ray sources (hot spots). More constraints on the azimuthal irradiation pattern of the accretion disk are expected from broader spectral coverage including the region of the Compton hump. The analysis presented here shows that some systematic dependencies of the reprocessed spectrum exist: A promising result is that the normalization of the observed Compton hump with respect to the soft X-ray continuum flattens toward the disk center at all

Table 1: Hard/soft X-ray slopes and equivalent widths of the iron $K\alpha$ -line for X-ray flares passing behind a black hole ($\phi = 180^\circ$). The spectra at the peak of the lightcurves are considered. Units: M in M_\odot , \dot{m}_{disk} in Eddington units, R in R_g , and equivalent widths in eV.

M	\dot{m}_{disk}	R	F_X/F_{disk}	primary	i	$\zeta_{\text{hs}}^{\text{loc}}$	$EW_{\text{loc}}(K\alpha)$	$\zeta_{\text{hs}}^{\text{far}}$	$EW_{\text{far}}(K\alpha)$
10^8	0.001	18	144	0	10°	0.46	1380	0.94	1595
10^8	0.001	18	144	0	30°	0.46	1570	0.94	1605
10^8	0.001	18	144	1	30°	0.20	250	0.21	80
10^8	0.001	18	144	0	60°	0.39	1580	0.88	1595
10^8	0.001	7	144	0	10°	0.72	2030	1.10	1730
10^8	0.001	7	144	0	30°	0.73	2070	1.12	1745
10^8	0.001	7	144	1	30°	0.21	245	0.29	135
10^8	0.001	7	144	0	60°	0.63	1950	1.16	1700
10^7	0.02	18	9	0	10°	0.59	1890	1.87	1865
10^7	0.02	18	9	0	30°	0.58	1880	1.83	1845
10^7	0.02	18	9	1	30°	0.21	255	0.21	70
10^7	0.02	18	9	0	60°	0.51	1740	1.67	1765

orbital phases. Additionally, the relativistic effects induce a phase-modulation of the reprocessing features. For a spot orbiting at $R = 10 R_g$, the deviation of the Compton hump maximum from its orbital average is up to 18%. Thereby, the hump's centroid shifts by up to 8%. In principle, observations from *Suzaku* and later from *Symbol-X*, *XEUS*, or *Constellation-X* can therefore further constrain position and motion of X-ray emitting spots co-orbiting with the disk.

By quantifying the re-processed spectra for a specific azimuthal phase of the orbiting hot spot we find that strong dependencies of $\zeta_{\text{hs}}^{\text{far}}$ and $EW_{\text{far}}(K\alpha)$ exist also on the global black hole parameters and on the intensity of the flare. Therefore it remains a multi-parameter problem to constrain the black hole properties and the irradiation pattern of the accretion disk. The consideration of variability data is a possibility to face this problem. Investigations of the power spectral density of AGN can successfully constrain the black hole mass (e.g. McHardy et al. 2005). We also expect further constraints on the black hole spin and on the irradiation pattern of the disk from our *rms* modeling (Goosmann et al. 2006) when applied to a broader spectral range.

Acknowledgements. We are grateful to Anne-Marie Dumont and Agata Różańska for their help computing the local spectra and the vertical disk profiles.

References

- Czerny, B., Różańska, A., Dovčiak, M., Karas, V., & Dumont, A.-M. 2004, A&A, 420, 1
Dovčiak, M. 2004, PhD-thesis, Charles University Prague, astro-ph/0411605
Dovčiak, M., Karas, V., & Yaqoob, T. 2004, ApJS, 153, 205
Dumont, A.-M., Abrassart, A., & Collin, S. 2000, A&A, 357, 823
Dumont, A.-M., Collin, S., Paletou, F., Coupé, S., Godet, O., & Pelat, D. 2003, A&A, 407, 13
Galeev, A. A., Rosner, R., & Vaiana, G. S. 1979, ApJ, 229, 318
Haardt, F., Maraschi, L., & Ghisellini, G. 1994, ApJL, 432, L95
Haardt, F., & Maraschi, L. 1991, ApJL, 380, L51
Iwasawa, K., Miniutti, G., & Fabian, A. C. 2004, MNRAS, 355, 1073
Goosmann, R. W. 2006, PhD thesis, Universität Hamburg
Goosmann, R. W., Czerny, B., Mouchet, M., Ponti, G., Dovčiak, M., Karas, V., Różańska, A., & Dumont, A.-M. 2006, A&A, 454, 741
Kaastra, J. S., et al. 2004, A&A, 422, 97
McHardy, I. M., Gunn, K. F., Uttley, P., & Goad, M. R. 2005, MNRAS, 359, 1469
Ponti, G., Cappi, M., Dadina, M., & Malaguti, G. 2004, A&A, 417, 451
Różańska, A., Dumont, A.-M., Czerny, B., & Collin, S. 2002, MNRAS, 332, 799
Turner, T. J., Miller, L., George, I. M., & Reeves, J. N. 2006, A&A, 445, 59